Paper Number

3D-Simulation of DI-Diesel Combustion applying a Progress Variable Approach accounting for Complex Chemistry

R.Steiner, C.Bauer, C.Krüger, F.Otto
DaimlerChrysler AG

U.Maas
Institut für Technische Thermodynamik, University of Karlsruhe

ABSTRACT

A progress variable approach for the 3D-CFD simulation of DI-Diesel combustion is introduced. Considering the Diesel-typical combustion phases of auto-ignition, premixed and diffusion combustion, for each phase, a limited number of characteristic progress variables is defined. By spatial-temporal balancing of these progress variables, the combustion process is described. Embarking on this concept, it is possible to simulate the reaction processes with detailed chemistry schemes. The combustion model is coupled with a mesh-independent Eulerian-spray model in combination with orifice resolving meshes. The comparison between experiment and simulation for various Diesel engines shows good agreement for pressure traces, heat releases and flame structures.

INTRODUCTION

Concerning the development of future internal combustion (IC) engines, the automotive industry is searching for new approaches to shorten the classical procedure of trail and error **[22]**. The rapid increase of computing power enables the 3D simulation of reactive in-cylinder flow dynamics as an increasingly valuable tool for combustion designers. In this paper, a CFD concept for the simulation of DI-Diesel engine combustion is introduced, complying with industrial requirements, such as a high degree of predictability and economical computational costs. The proposed approach allows the incorporation of complex chemistry into a detailed turbulent flow prediction.

In order to overcome the well-known drawbacks of conventional stochastic spray models in the near nozzle region, an Eulerian approach in combination with orifice resolving meshes is applied to improve predictability. For the numerical simulation of the Diesel combustion process, a limited number of appropriate progress variables are defined to describe the reactive phases of self-ignition, premixed and diffusion combustion. For each progress variable, a transport equation is solved in the CFD code. The mixture field in physical space is characterised by the mixture fraction and its variance. By weighting the chemical solution in mixture fraction space with a presumed probability density function (pdf), the transport equations for each progress variable in physical space are closed.

The introduced progress variable approach offers a way of separating the numerical effort associated with the solution of the turbulent flow field from that of solving the chemistry. Thereby, arbitrarily complex chemistry can be used to simulate the reactive processes.

In this study, the progress variable approach is applied to simulate the combustion process in a passenger car heavy duty truck and marine engine for different operation conditions.

MODEL FORMULATION

In this section an integrated numerical model for the simulation of Diesel combustion is introduced which was developed to meet the essential industrial demands both a high degree of predictability and low CPU costs. To realize such a model, a compromise between the level of detail for modeling and the computational effort has to be found. Relevant influence parameters have to be identified and modeled. In addition, all approaches should preferably have the same level of details since the weakest sub-model determines the predictive capability.

The reliable simulation of mixture formation is a crucial prerequisite for the simulation of combustion in IC engines. Due to strong mesh dependence, 3D-simulation of Diesel sprays applying a pure Lagrangian approach usually is not even capable to predict global quantities like penetration length of liquid and vapor. The main reason for this shortcoming is the insufficient numerical resolution of the flow near the orifice. Therefore, for this study an Eulerian spray model **[1]** in

combination with adaptively refined meshes in the spray region is used to overcome this deficits.

For the modeling of the Diesel combustion process a progress variable approach **[2]** is used. Representative progress variables are identified to describe the chemical reactive phases of self-ignition, premixed and diffusion combustion. For the simulation of the auto-ignition process, a library-based detailed chemistry scheme is applied **[3]**. Additionally, a concept is introduced which accounts for cool flame effects **[4]**. This is especially important when studying "Homogenous Charge Compression Ignition" (HCCI) engines. The combustion model **[2]** based on the PDF-Timescale Model **[8,9]** which itself represents a combination of the Characteristic-Timescale Model **[11]** and the Flamelet Model **[6]**. This *hybrid* combustion model covers the phases of premixed and diffusion combustion and its transition. In this paper a new concept for combustion modeling is introduced which differs from the PDF-Timescale Model in such a way that no flamelet based library is needed and the solution of the chemical time-scales are based on detailed chemistry computations.

In order to account for turbulent mixing effects, a presumed probability density function is used whose shape is defined by the mean and the variance of a conserved scalar. Further details of each model are given below.

SPRAY MODELLING

The reliable simulation of mixture formation is a crucial prerequisite for the simulation of combustion and pollutant formation in DI Diesel engines. In almost all commercial and university IC engine codes a Monte Carlo method is used which resolves discontinuous droplet processes like turbulent dispersion, droplet breakup and droplet collisions in a stochastic way. There are four main problems related to the application to IC engines:

1. Large differences in relevant length-scales (DC heavy duty truck engine: bore 13 cm, effective nozzle diameter 200μm) make it difficult to resolve the flow near the nozzle orifice which leads to substantial grid dependence **[19]**. The velocity profile of the gas phase cannot be resolved and relative velocities between the droplets and the gas phase are over-predicted (see ***fig.1***). Therefore the exchange processes between the phases are not accurately calculated, independent of the quality of the sub-models **[13]**.

2. Even though in the future CFD meshes might be able to resolve the orifice (e.g. by spray adapted meshing strategies) the stochastic approach would run into convergence problems with the droplet-pdf. While the mesh size is decreased to improve the (spatial) resolution of the flow, the number of "parcels" per CFD cell (which is a measure of the resolution of the droplet statistics) decreases. Consequently, the number of "parcels" for the whole calculation also has to be increased; a huge number of "parcels" is required. Due to the stochastic character of this method, the number of parcels per cell cannot be controlled. Especially collision models which are based on two point correlation cannot be applied at al independently of the modeling approach

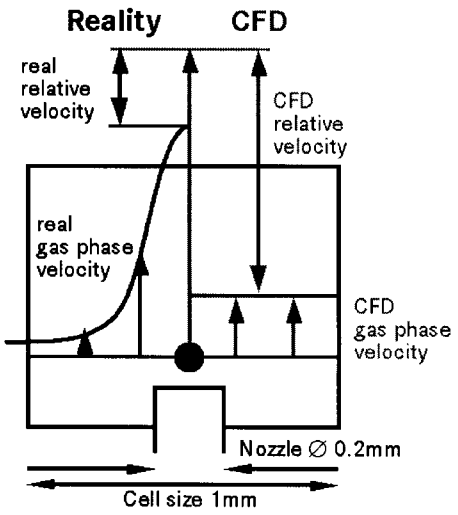

Figure 1: The relative velocity between droplets anc gasphase is overpredicted on meshes which do no resolve the orifice.

3. Turbulence is modeled on a different level of detail foı the gas phase and the droplets. For engine applications, the Navier Stokes equations have to be used in an ensemble averaged form. Such ar averaging procedure is not done for the disperse phase. Its turbulent fluctuations are resolvec stochastically by the local parcel ensemble, based or the Langevin equation. Due to the limited number o parcels per cell, results are be obscured by statistica noise.

4. Physical processes especially in the near-nozzle region are poorly understood. The influence o turbulence and cavitation on the spray disintegratior into droplets is unclear. Of course, to be able tc investigate different physical sub-models, steps 1. - 3. have to be solved first to provide a consisten numerical basis.

Intensive research was done at DC to avoid the problems discussed above. In this paper, the so called ICAS (Interactive Cross section Averaged Spray) model is used, where in the near-nozzle region, the governing equations are integrated over the spray cone **[20]**. This one-dimensional spray model (where the relevant length scales are automatically resolved) is coupled interactively with the CFD code via source terms in the balance equations. The moments of the droplet-pdf are resolvec by several droplet classes in Eulerian coordinates. The

governing transport equations for droplet mass, momentum, surface area and temperature are presented in detail in **[1]**. Boundary conditions for the integral mass and momentum fluxes as well as for initial droplet size and velocity distributions are taken from simulation of the cavitating nozzle flow. The used nozzle flow model has already been validated against measurements in optical accessible multi-hole real-size nozzles **[15]**. Further downstream it is switched over to the stochastic spray model. In combination with a so-called "length scale limiter" **[14]** and adaptively refined meshes in the spray region almost mesh independent results could be achieved **[16]**. ***Fig.2*** illustrates the introduced spray modeling concept.

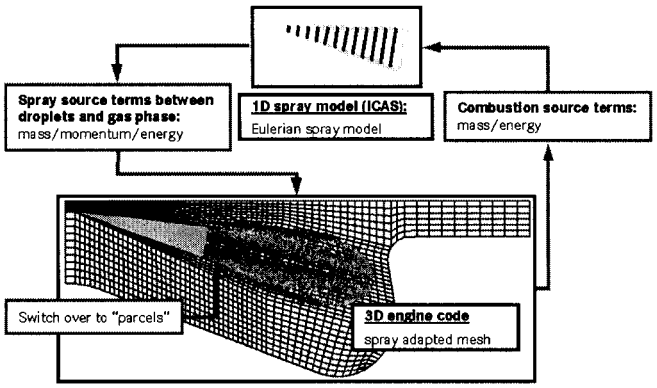

Figure 2: Concept of ICAS. The 1D spray model is coupled interactively with the CFD engine code. Spray adapted meshes are used to achieve mesh independent results.

SOME GENERAL ASPECTS ABOUT DIESEL COMBUSTION MODELING

Diesel combustion is the result of complex, closely coupled physical and chemical processes. Therefore, to model Diesel combustion, the effects of turbulence on the mean reaction rates has to be considered. Two main effects can be distinguished:

Heterogeneous mixture field distribution

Particularly in the early injection phase, spray-induced turbulence leads to a highly non-homogenous mixture field. Typically, in Reynolds-averaged-Navier–Stokes (RANS) models the mean values of the fluid quantities are calculated. For this reason - depending on the spatial discretisation of the combustion chamber – information on local mixture inhomogeneities gets lost. ***Fig.3*** shows a comparison between a realistic and a corresponding computed ensemble-averaged mixture field. Due to the dependence of chemical reactions on the mixture, it is evident, that combustion models which consider only mean values can lead to miscalculations. Besides the inhomogeneity of the mixture, the turbulent distribution of the thermodynamic quantities can play a crucial role.

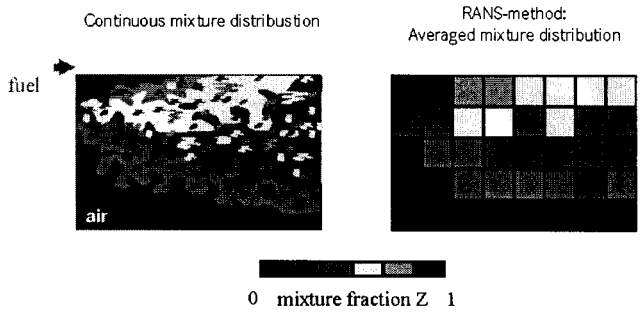

Figure 3: Exemplary comparison between a realistic anc a computed mixture between air (Z=0) and fuel (Z=1).

Turbulence-chemistry interaction:

Turbulent and chemical time-scales vary by severa orders of magnitude in turbulent combustion, where the chemical time-scales typically span a much broader range than the physical ones. In ***fig.4*** a comparison is giver between time-scales occurring in turbulent reactive flows. The reaction rates are always controlled by the slowest processes. Depending on the time-scale ranges, three scenarios can be distinguished:

1. $\tau_{chem} \approx \tau_{turb}$: Turbulence- and chemistry-controlled
2. $\tau_{chem} >> \tau_{turb}$: Chemistry-controlled (e.g. Diesel premixed combustion)
3. $\tau_{chem} << \tau_{turb}$: Mixing-controlled (e.g. Diesel diffusion combustion)

Depending on the chemical time-scale range, the mathematical description of chemical processes can be classified into kinetic and thermodynamic equilibrium approaches (see ***fig.4***). In order to keep the computational costs low, equilibrium approaches should be always preferred as long as they are valid.

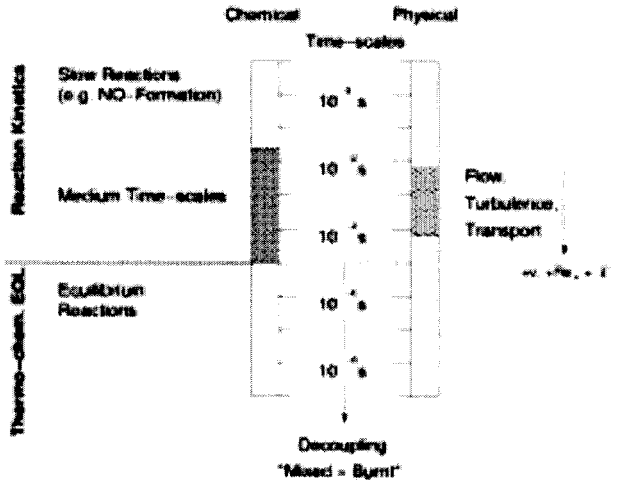

Figure 4: Time-scale range of turbulent, reactive flows (cf. **[6]**).

When the Diesel combustion is fully developed, we find the so-called diffusion combustion regime which is *mixing-controlled*. At least the main chemical reactions (which are responsible for the heat release) are much faster than the mixing. Therefore, the mixing process is dominant and directly determines the local chemical states.

Especially for a reliable simulation of *chemically-controlled* combustion processes, it is necessary to incorporate detailed chemical mechanisms, which include many hundreds of reactions and also a very large number of species. The spatial-temporal development of each species is determined by a non-linear differential equation. Just to solve the whole set of equations for each computational cell would not be a reasonable approach: the CPU need would be too high and the turbulent substructure would be neglected. More eligible approaches offer *flamelet type models* in conjunction with presumed shaped probability density functions. The basic idea of these models is the separation of the fluid dynamic calculation from that of the chemistry. By introducing the mixture fraction as conserved scalar, the three-dimensional problem in physical space transforms to an one dimensional problem in mixture fraction space. The mixture fraction describes the mixing state of two streams and takes values between 0 and 1. The reduction of dimensionality enables the application of detailed chemical mechanism without imposing a significant penalty on computational time. A comprehensive overview of flamelet models is given in **[7]**. In the context of this paper the flamelet approach is used not only in the classical way but also for local laminar combustion scenarios.

Under the assumption of fast chemistry, in the laminar flamelet concept a turbulent flame is considered as an ensemble of 1D-laminar diffusion flamelets. Introducing the mixture fraction as independent coordinate, Peters **[7]** has derived the laminar flamelet equations. A local coordinate transformation is used to transform the balance equations for enthalpy and species into mixture fraction space. The flamelet equations for the species mass fractions y_i read as follow:

$$\rho\frac{\partial y_i}{\partial \tau} = \rho\frac{\chi}{2Le_i}\frac{\partial^2 y_i}{\partial Z^2} + \dot{y}_i^c \,, \qquad (1)$$

where $Z, \tau, Le_i, \dot{y}_i^c$ denote the mixture fraction, the time in Z-space, the Lewis number and the chemical production rate of species i. The scalar dissipation rate χ represents instantaneous local diffusion and strain effects by the flow field **[7]**. In order to obtain the mean mass fractions of species i in physical space $\tilde{y}_i(\vec{x},t)$ (which are used e.g. for the closure of the turbulent flow quantities), the current laminar flamelet solutions $y_i(\tau, Z, \chi)$ are weighted with a presumed-pdf for the mixture fraction $\tilde{P}_Z$:

$$\tilde{y}_i(\vec{x},t) = \int_Z y_i(\tau, Z, \chi)\tilde{P}_Z(Z;\vec{x},t)\,dZ \qquad (2)$$

For the mixture fraction Z, the β-function pdf is widely used which is defined by just two parameters, e.g. the mean value $\tilde{Z}$ and its variance $\tilde{Z}''^2$ (see e.g. **[5]**):

$$\tilde{P}_Z(Z;\vec{x},t) = \gamma \cdot Z^{\alpha-1}(1-Z)^{\beta-1} \quad (\gamma = \text{norm. factor}) \qquad (3)$$

Thus, to calculate the β-function pdf, two additiona transport equations have to be solved in the CFD-code:

$$\frac{\partial(\rho\tilde{Z})}{\partial t} + \nabla\cdot(\rho\tilde{u}\tilde{Z}) = \nabla\cdot\left[\frac{\mu}{Sc_{\tilde{Z}}}\nabla\tilde{Z}\right] + \tilde{\rho}^s \qquad (4)$$

$$\frac{\partial(\rho\tilde{Z}''^2)}{\partial t} + \nabla\cdot(\rho\tilde{u}\tilde{Z}''^2) = \nabla\cdot\left[\frac{\mu}{Sc_{\tilde{Z}''^2}}\nabla\tilde{Z}''^2\right] + \frac{2\mu}{Sc_{\tilde{Z}''^2}}(\nabla\tilde{Z})^2 - \rho\tilde{\chi} + \tilde{\rho}^s \qquad (5)$$

Fig.5 shows several mixture distributions in Z-space which can be resolved with the β-pdfs.

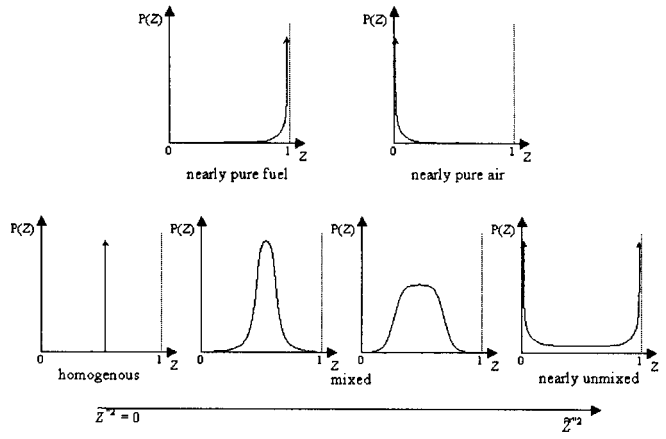

Figure 5: Examples of β-pdf shapes.

Recent results obtained using pdf-modeling based or the solution of the pdf transport equation, show that ir spray combustion the shapes of the pdfs can differ remarkably from β-functions. Therefore further research is needed to improve the description of the pdf-shapes.

For the implementation of flamelet type models in CFD several ways are possible, which differ by their

1. Level of detail for the solution of the flamelet equations (cf. eq. 1) where
   - unsteady $y_i(\tau, Z, \chi)$ and steady $y_i(Z, \chi)$
   - diffusive $y_i(\tau, Z, \chi)$ and non-diffusive $y_i(\tau, Z)$
   - and detailed $y_i(\tau, Z, \chi)$ and equilibrium chemistry $y_i(Z)$

   flamelets can be distinguished.

2. Description of the interaction between fluid dynamics and flamelets
   - Post-Flamelets: CFD → flamelets
     → e.g. species concentrations
   - Interactive Flamelet(s): CFD ↔ flamelet(s):
     → species concentrations
     → reaction rates

Assuming equilibrium chemistry for the flamelet solution implies automatically no time nor transport dependency of the flamelets. Thus, implementation is simplified and the CPU need is reduced. However, this is purchased by neglecting important physical and chemical effects. For "non-diffusive flamelets", the flamelet equations transform into conservation equations for homogenous reactors. Concerning the interaction between fluid dynamics and flamelets, the use of Post-Flamelets represents a pure Post-Processing application, so that combustion models are still necessary for the solution of the reactive fluid dynamics. Depending on the flamelet parameters (e.g. temperature, pressure, scalar dissipation rate,...) delivered by the CFD-code, species information in physical space can be calculated. For interactive flamelet concepts, an information exchange in both directions takes place. The CFD-code delivers the flamelet parameters. In return, the flamelet code results can be used to close the unclosed terms in the balance equations solved in the CFD-code. Depending on the chemical time-scales, it is advantageous to use as interaction quantities mass fractions or reaction rates.

PROGRESS VARIABLE APPROACH

As pointed out before, combustion designers are interested in CFD tools which deliver a maximum of predictable capability and at the same time a minimum of CPU costs. The progress variable approach represents a kind of compromise to meet this challenging goal. It attempts to describe complex chemical phenomena with a limited number of representative progress variables. Additionally to the commonly used conservation equations, for these chemical indicator species $\tilde{\Psi}_i$, the following conventional spatial-temporal transport equations have to be solved:

$$\frac{\partial(\rho\tilde{\Psi}_i)}{\partial t} + \nabla\cdot\left(\rho\tilde{u}\tilde{\Psi}_i\right) = \nabla\cdot\left[\frac{\mu}{Sc_{\tilde{\varphi}_i}}\nabla\tilde{\Psi}_i\right] + \tilde{\Psi}_i^c \quad (6)$$

Generally, the progress variable approach comprises two issues:

1. Identification of characteristic progress variables
2. Determination of mean chemical source terms to close eq.6.

Definition of progress variables

For the definition of an appropriate minimum number of progress variables, it is advantageous, to split the overall Diesel combustion process into several characteristic phases. Considering as example the heat release rate ***fig.6*** shows exemplary the subdivision as directed in this study. Three phases are distinguished:

- Ignition phase (chemistry-controlled)
- Premixed combustion (chemistry-controlled)
- Diffusion combustion (mixing-controlled)

In each of these phases different variables are suitable to describe the reaction progress, which will be discussed below.

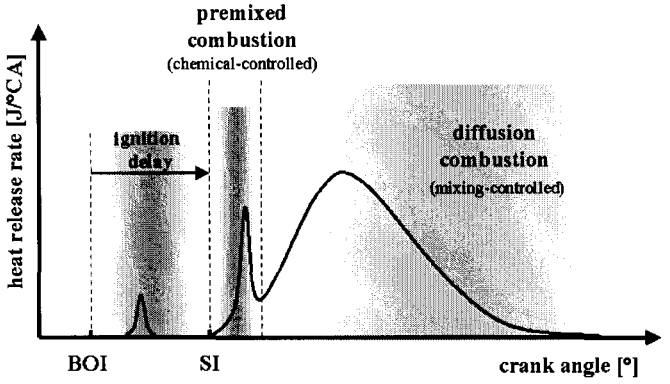

Figure 6: Zoning of the overall Diesel combustion process on the basis of the heat release rate.

Determination of the mean chemical source terms

As described above, flamelet type models offer a possibility to account for heterogeneous mixture distribution (→ pdf), turbulence-chemistry interaction (→χ) and the incorporation of detailed chemical reactions schemes (introduction of Z). Therefore in this study, flamelet type approaches are used, to model the mean chemical source terms, needed for the closure of the transport equations for each progress variable. It is tried to find solutions which keep the numerical effort within economical limits. Thus for example, detailed chemical schemes should only be used when they are needed. Additionally, the area of validity of the flamelet equations (see eq.1) (based on fast chemistry assumption!) is taken into consideration. Concerning numerical aspects, the performing of the integration in eq.2 plays a crucial role when using presumed pdf flamelet type concepts. In this study a semi-analytical method is used, based on the piece-by-piece integration

of the mixture fraction integrals which results in incomplete β-functions (see appendix A).

The models to simulate the auto-ignition and the combustion process are described in more detail in the next sections.

PDF IGNITION MODEL

Ignition model for conventional Diesel-Ignition

In this section an ignition model based on a framework of **[3]** is introduced to model the ignition process of conventional Diesel engines taking into account turbulent mixture field fluctuations. Due to the rapid ignition process which occurs in a typical Diesel operation mode (injection timing close to TDC), the heat release during the ignition delay period is neglected. The concept follows the progress variable approach, so that at first an appropriated ignition indicator species has to be defined.

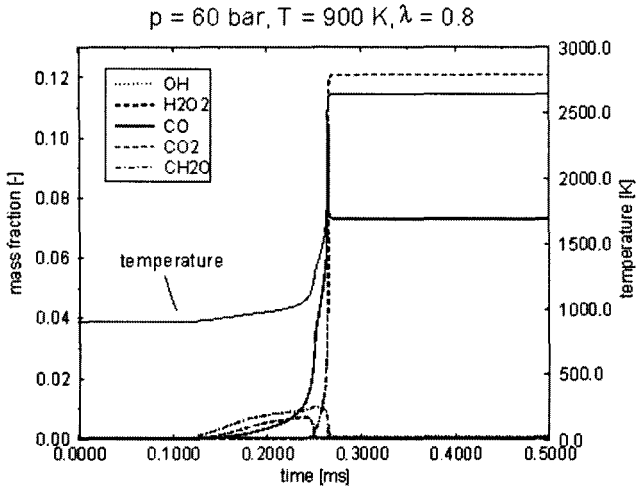

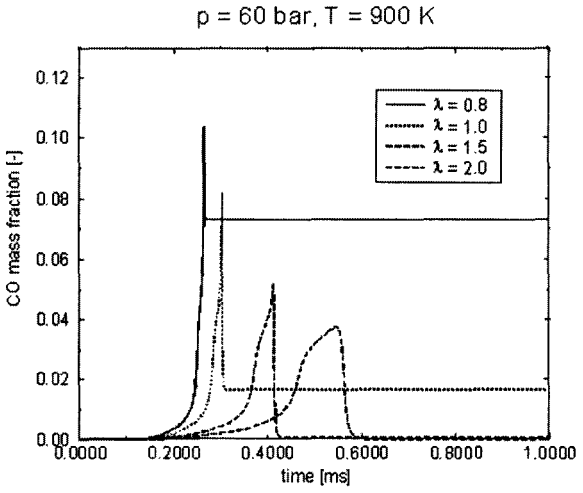

Figure 7: Constant pressure studies which show the monotonous formation behavior of CO during the ignition phase.

As a basic requirement, this variable must have a monotonous formation behavior during the ignition period. For the identification, homogeneous reactor calculations based on detailed chemistry were carried out. ***Fig.7*** shows exemplarily, that carbon-monoxide (CO) fulfills this requirement quite well. Its monotonous behavior ends with the beginning of the main combustion when CO is reduced rapidly.

The spatial-temporal development of the progress variable CO is handled passively in the CFD-Code using the common transport equation eq.6. The challenging task is again the closure of this equation with the mean chemical source term.

It is well known that the reactivity of a system depends strongly on the temperature and the fuel concentration. Therefore it is essential to find the physical correlation between these two parameters. This is done with the following mixture fraction approach, based on two streams (see ***fig.8***).

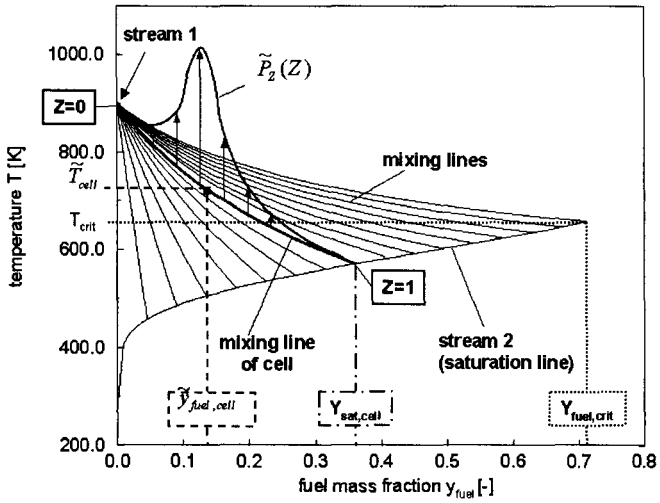

Figure 8: Pdf-integration concept based on mixing lines to get the correlation T(Z).

The first stream consists of fresh air (and burnt gases in the case of EGR). The second one is characterized by fuel in the saturated condition, which can be found in the vicinity of the droplets. This implies the assumption, that droplets are still existent during the ignition process. Knowing the molar mass of fuel M_{fuel}, the molar mass of the mixture without fuel M_{mix} and the existing pressure p_{cyl} in the combustion chamber, it is possible to calculate the saturation line (which corresponds to stream 2) given by the following thermodynamical relation:

$$y_{fuel}(T) = \frac{M_{fuel}}{M_{fuel} + M_{mix} \cdot \left(\frac{p_{cyl}}{p_{vap}(T)} \right)} \qquad (7)$$

p_{vap} is the vapor pressure of the fuel. In combination with an enthalpy balance it is now possible, to calculate the mixture lines between the upper left point of pure air and the corresponding points on the saturation line. The temperature of the point of stream 1 is an average value of the regions in the combustion chamber without fuel.

In order to account for the turbulent mixture distributions, again the β-pdf is used (see eq.3), where the mean mixture fraction $\widetilde{Z}^*$ is defined as:

$$\widetilde{Z}^* = \frac{\widetilde{y}_{fuel}}{y_{sat}} \quad , \widetilde{Z}^* \in [0,1] \qquad (8)$$

y_{sat} represents the saturated condition of fuel which is determined by the corresponding mixing line (see ***fig.8***). It shall be noted here that this simple model cannot account for deviations from the phase equilibrium. The inclusion of such processes is the topic of future work. For each computational cell, with $\widetilde{T}_{cell}$ and $\widetilde{y}_{fuel,cell}$, the corresponding temperature distribution T(Z) can be quantified. Now the mean reaction rate $\dot{\omega}_{CO}$ can be calculated using the following pdf-integration:

$$\widetilde{\dot{\omega}}_{CO}(\vec{x},t) = \int_0^1 \dot{\omega}_{CO}(Z, p, T(Z), y_{co}, egr) \cdot \widetilde{P}_Z(Z;\vec{x},t)\, dZ \qquad (9)$$

where $\dot{\omega}_{CO}$ is the laminar reaction rate of CO. The values of $\dot{\omega}_{CO}$ depend on the mixture fraction Z, pressure p, temperature T, mass fraction y_{CO} and the egr-ratio. For this study, a library for $\dot{\omega}_{CO}$ was generated, based on isobar homogenous reactor calculations using a detailed n-heptane mechanism **[17]**. The initial conditions of the reactors were varied in p-, T-, y_{fuel} and egr-space. Each calculation was tabulated in terms of equidistant CO mass fractions. The pressure variation span between 20 to 200 bar in 20 bar steps, while the temperature was divided in 20 K steps starting at 700 K and ending at 1500 K. In each point of the library the corresponding reaction rate of CO was tabled. For the numerical solution of eq.9 the semi-analytical method described in appendix A can be applied.

The transition from the ignition to the combustion model is done, when the mass fraction of the indicator species exceeds a pre-defined limit of 0.02, which is an empirica value resulted from a sensitivity analysis based or homogenous reactor calculations.

This model still contains the drawback that the CO mass fraction is assumed to be constant in mixture fractior space. To overcome this drawback, a new concept for a turbulent ignition model is explained consecutively.

Concept of an advanced ignition model including HCCI-ignition processes

The ignition model explained above is only valid for conventional Diesel ignition with fast ignition processes and negligible heat transfer rates during the inductior phase. These conditions are not fulfilled in the case o HCCI ignition where especially cool flames contribute up to 10% to the overall heat release **[18]**. Also high EGF rates increase the ignition delay whereas the initia reactions contribute to the heat release during the ignition phase.

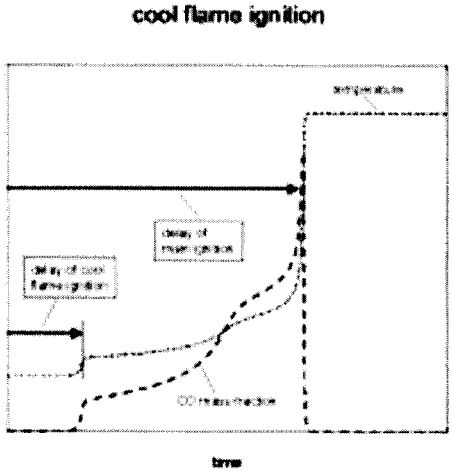

Figure 9: Typical behavior of cool flame ignition

In ***fig.9*** a typical homogenous reactor calculatior including cool flames is shown. The time development is characterized by a long delay up to the step of the coo flame. After the cool flame there is another part of the ignition process with low reactivity which ends with the start of the main ignition. Having a look at the CO mass fraction, the monotonous behavior of CO is still existent But a big problem is the first ignition delay up to the star of the cool flames, which cannot be characterized by the CO mass fraction, as there is no significant CC production. This makes it impossible to use the CO as progress variable under such conditions. Anothei variable has to be found.

The basic requirement for a suitable progress variable is the ability to capture especially the long ignition delay up to the start of the cool flames. A possible parameter fulfilling this criteria is the reaction time t_{reac}, meaning the

time from start of the reaction up to the actual time. Two assumptions are important concerning the modeling:

- The start of the reaction process ($t_{reac} = 0.0$) for all the conditions in the mixture fraction space of a cell is simultaneous.
- All the conditions in the mixture fraction space of a cell have the same temporal development of t_{reac}.

The big advantage of this approach is the fact, that no pdf is needed for the description of the reaction time, as it is a global scalar of each cell. In other words: Each condition within the mixture fraction space of a cell sees the same reaction time t_{reac}.

The model works in the way, that the reaction time of each cell is handled as a passive scalar and is transported via a transport equation considering convection and diffusion. The challenge is the closure of the diffusion and spray source term. The reaction time in a cell is started, when a predefined minimum amount of the global fuel mass fraction is exceeded within a cell.

With the objective to calculate the mean heat release rate $\tilde{\dot{q}}$ (see eq.10), the distribution of the laminar heat release rates $\dot{q}(Z)$ in mixture fraction space have to be specified. This is done using tabled (or online calculated) laminar heat release rates taken out of homogenous reactor calculations, which correlate with the reaction time t_{reac} of the cell. The pdf-integration then is similar to the one already described, using the mixing line to get the correlation T(Z). The so calculated turbulent heat release rate then is coupled to the energy equation of the 3D-Code.

$$\tilde{\dot{q}}(\vec{x},t) = \int_0^1 \dot{q}(Z,p,T(Z),t_{reac},egr)\cdot \tilde{P}_Z(Z;\vec{x},t)\,dZ \qquad (10)$$

Another difficulty arises in considering the chemical development of the species in the 3D-Code. Since the combustion model introduced below is based on seven species, it is not possible to model the detailed progress of the species equal to the behavior in the detailed chemical mechanism used to generate the library. Instead of this the available seven species develop depending on the amount of released energy toward their chemical equilibrium.

The switch from the ignition model to the combustion model is done depending on the released energy of each cell. Therefore a transport equation for the released energy is introduced. This amount of energy is compared with the theoretical amount of the overall heat release of the cell. If the ratio exceeds 10%, the cell is assumed to be ignited and the combustion model is activated.

7-SPECIES PDF-TIMESCALE MODEL

One challenging task in combustion modeling is the closure of the species conservation equations (see eq.6) with the mean reaction rate terms. In this section a model is introduced which attempts to capture both modes of Diesel combustion (and its coupling), the chemistry-controlled premixed and the mixing-controlled diffusion combustion phase. The so-called 7-Species PDF-Timescale Model model **[2]** based on the PDF-Timescale Model **[8,9]** which itself represents a combination of the Characteristic-Timescale Model **[11]** and the Flamelet Model **[6]**. As mentioned above, the flamelet model is just valid where the chemical time-scales are smaller than the turbulent time-scales. In order to expand the flamelet solution to low Damköhler number regions, the PDF-Timescale Model combines the flamelet solution with a time-scale approach. The time rate of change of species i is then given as:

$$\frac{\partial \tilde{y}_i}{\partial t} = -\frac{\tilde{y}_i - \tilde{y}_i^*}{\tau_{chem}} \qquad (11)$$

where $\tilde{y}_i^*$ is the value of the mass fraction obtained from eq.2 assuming a steady state flamelet solution. An expression for the mean mass fraction of species *i* at time n+1 is given by integrating eq.11 assuming that the coefficients remain constant during that time step:

$$\tilde{y}_i^{n+1} = \tilde{y}_i^* + \left(\tilde{y}_i^n - \tilde{y}_i^*\right) e^{-\frac{\Delta t}{\tau_{chem}}} \qquad (12)$$

The second term in eq.12 can be interpreted as a perturbation added to the steady flamelet solution.

In this study, the laminar flamelet solution in eq.2 is assumed to represent thermodynamic equilibrium, such that $y_i^* = y_i^*(T, p, Z)$. According to the Mixing-Timescale Model **[10]** only seven species are considered - fuel, O_2, N_2, CO_2, CO, H_2, H_2O - which are necessary to predict thermodynamic equilibrium temperatures accurately. Therefore, the seven species can be viewed as kind of progress variables to describe the heat release. In ***fig.10***, for an exemplary thermodynamic and mixture state, the 7 species mass fractions are plotted over the mixture fraction. Additionally, depending on $\widetilde{Z}''^2$ three shapes of the β-pdf are depicted. ***Fig.10*** points up a big benefit of the 7 Species-PDF-Timescale Model against e.g. the Mixing-Timescale model: Heterogeneous mixture distributions, which are described by $\widetilde{Z}''^2$ are taken into account for the calculation of the mean chemical reaction terms. For $\widetilde{Z}''^2 = 0$, the 7-Species-PDF Timescale Model complies with the Mixing-Timescale Model. For the numerical solution of eq.2, the semi-analytic method (see appendix A) is for the 7-Species-PDF-Timescale model well-suited since the *linearisation* of $y_i^* = y_i^*(T, p, Z)$ can be done with few discretisation points.

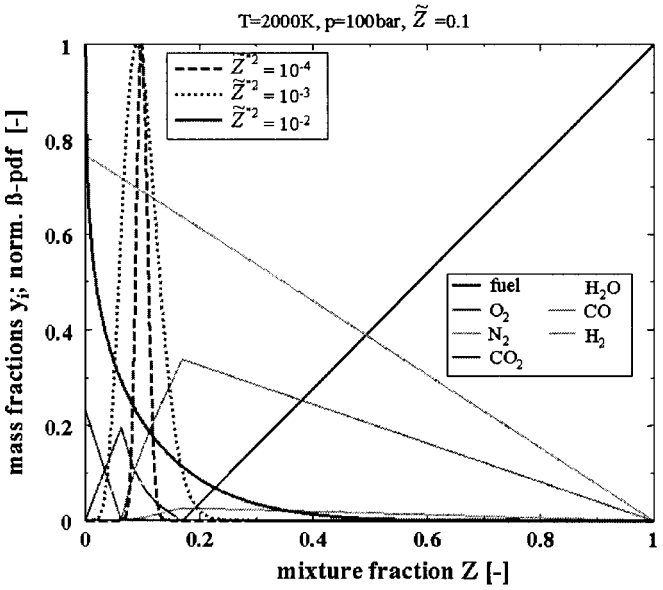

Figure 10: The equilibrium solution of the species mass fractions for an exemplary mixture and thermodynamic state as a function of the mixture fraction. Additionally, for three different $\widetilde{Z}''^2$ the corresponding β-pdfs are shown which transform the mixture inhomogenities from physical to chemical space.

An important aspect for the solution of eq.11 is the determination of the characteristic chemical time-scale. τ_{chem} represents the rate, at which each species approaches its equilibrium value. Currently, to simplify mass conservation issues a single time-scale is assumed which is based on a single step reaction for Diesel combustion:

$$\tau_{chem} = A^{-1} \cdot \left(y_{C_{14}H_{30}}\right)^{0.75} \left(y_{O_2}\right)^{-1.5} e^{\left(\frac{E}{RT}\right)} \qquad (13)$$

where in **[10]** for tetradecane $A = 1.54e^{10}\ s^{-1}$ and $E = 77.3$ kJ/mol are proposed. These values represent empirical quantities which need problem-specific adaptation.

Concept of an advanced 7-Species PDF-Timescale Model accounting for complex chemistry

With the intention of a more physical modeling of τ_{chem} in **[2]** a new approach is suggested which allows for incorporation of detailed reaction kinetics. This is particularly important, for the simulation of the chemical-controlled premixed combustion phase.

The model is based on the introduction of a mean reaction progress variable c

$$\widetilde{y}_i^{n+1} - \widetilde{y}_i^n = c\left(\widetilde{y}_i^* - \widetilde{y}_i^n\right), \qquad (14)$$

where the limiting value $c = 0$ describes no reaction ($\widetilde{y}_i^{n+1} = \widetilde{y}_i^n$) and $c = 1$ complete reaction ($\widetilde{y}_i^{n+1} = \widetilde{y}_i^*$). The comparison between eq.12 and eq.14 leads to an expression for c:

$$c = 1 - e^{-\frac{\Delta t}{\tau_{chem}}} \qquad (15)$$

which includes two unknowns, the characteristic chemical time-scale τ_{chem} and the elapsed reaction time Δt. At first, we concentrate on the determination of τ_{chem}. Therefore, we transform eq.15 in laminar mixture fraction space:

$$c(Z) = 1 - e^{-\frac{\Delta t}{\tau_{chem}(Z)}} \qquad (16)$$

$\tau_{chem}(Z)$ represents the timeframe needed to reach a predefined reaction progress criterion. In order to determine $\tau_{chem}(Z)$, homogenous reactor calculations can be used. ***Fig.11*** illustrates schematically the procedure: The normalized temperature progression serves as progress variable. Depending on a specific progress criterion $\tau_{chem}(Z)$ can be quantified for each homogenous reactor.

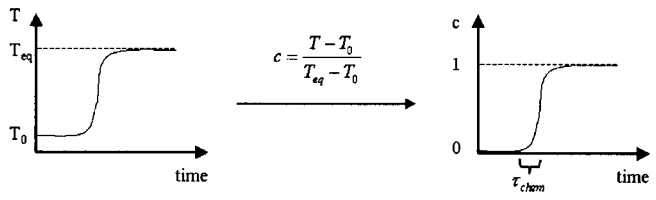

Figure 11: Procedure to determine the laminar chemical time-scale.

In order to calculate the mean reaction progress $\tilde{c}$, its instantaneous values $c(Z)$ are weighted with a β-pdf. The different heat releases have to be accounted for:

$$\tilde{c} = \frac{\int_Z c(Z) \cdot \Delta H(Z) \cdot \tilde{P}_z(Z;\vec{x},t)\, dZ}{\int_Z \Delta H(Z) \cdot \tilde{P}_z(Z;\vec{x},t) dZ} \qquad (17)$$

where $\Delta H(Z)$ represents the heat release of each homogeneous reactor. In order to solve eq.17, the reaction time Δt still needs to be defined. Δt indicates the elapsed reaction timeframe. It can be quantified be solving a transport equation in the CFD-code.

RESULTS

In order to evaluate the models developed in this study, various Diesel engines were simulated, including a passenger car, heavy duty truck and marine engine. Both, the passenger car and the marine engine are equipped with a Common-Rail (CR) injection system, whereas the heavy duty truck engine is set up with a Pump-Line-Nozzle (PLN) system. Several operating conditions have been investigated.

For the validation of the combustion models, the measured cylinder pressures are used. The pressure data were obtained with single-cylinder engines. Additionally, heat release curves are compared which results from zero-dimensional heat release calculations based on the pressure traces. For the spatial characterization of mixture formation and combustion of the heavy duty truck engine, at DaimlerChrysler a single cylinder optical engine has been set up, allowing full optical access to the combustion chamber, for e.g. high speed photography. Photographic sequences of combustion processes are used to compare the flame front propagation between simulation and experiment.

For the simulation of the engine cases the ICAS model was coupled with the introduced progress variable approach using KIVA3v **[21]** as CFD-code. In the transport equation for the variance of the mixture fraction the spray source term is neglected. The ignition model uses CO as progress variable (section: *Ignition model for conventional Diesel-Ignition*). For this study, the chemical time-scale of the introduced 7-Species-PDF-Timescale-Model is based on the single step reaction of eq.13 whereas the empirical parameter *A* needs problem-specific adaptation. In ***fig.12*** the influence of *A* is illustrated in form of calculated pressure traces for the half load case of the heavy duty truck engine. For obvious reasons *A* influences the premixed combustion phase because it is primarily chemically controlled on account of low temperature levels. Since *A* represents an inverse time-scale, the increasing of *A* leads to a faster premixed combustion. In addition, the peak pressure is slightly increased and the occurrence of peak pressure is minimal shifted towards earlier crank angles. It is obvious that for combustion processes with short premixed combustion phases (full load operation conditions) the influence of *A* loses weighting.

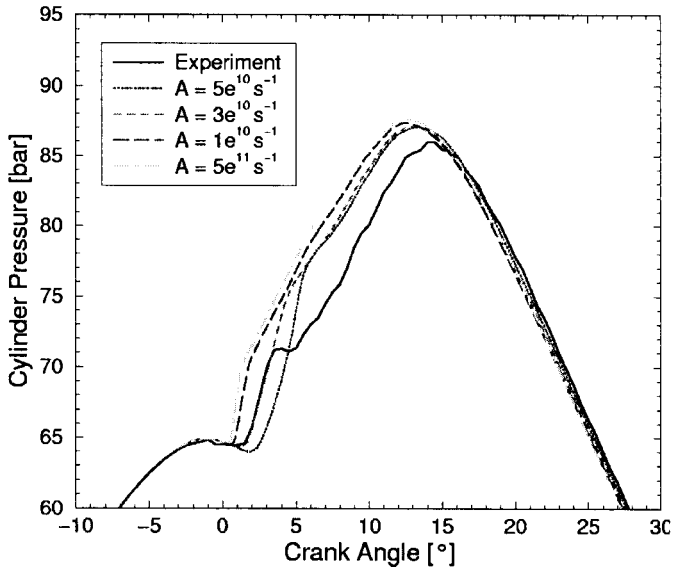

Figure 12: Sensitivity of the combustion process relating to the chemical time-scale based on the single step reaction: $\tilde{\tau}_{chem} = A^{-1} \cdot \left(y_{C_{14}H_{30}}\right)^{0.75} \left(y_{O_2}\right)^{1.5} e^{\left(\frac{E}{RT}\right)}$.

Based on symmetry considerations only sector meshes were modeled. This leads to a significant reduction of the computational effort. To ensure a grid-independent solution of the gaseous phase of the engine code, an adaptive mesh refinement of the engine grid in the spray region was applied.

Fig.13 shows the comparison between measured and predicted ignition delays for the heavy duty truck engine. Load and engine speed variations are considered. By keeping the pre-exponential factor *A* of the chemical time-scale constant, the ignition delays match within the bounds of one degree crank angle.

***Fig.14*-18** show a comparison of measured and calculated cylinder pressures and heat release rates. Additionally, the total heat releases are depicted. It can be seen that the simulation matches the experimental

pressure and heat release curves very closely. The major features of combustion including ignition delays, occurrence and order of peak pressures and expansion pressures are captured accurately.

Premixed combustion is slightly over-predicted which causes mostly a lacking energy release in the late diffusion combustion phase. To predict the chemically controlled premixed combustion phase more accurate, the introduced *concept of an advanced 7-Species-PDF-Timescale-Model accounting for complex chemistry* is promising since it allows the incorporation of detailed reaction kinetics. Furthermore, it is needed to improve the description of the pdf-shapes which describe local mixture distributions. Concerning the β-pdf this comprises among other things the modeling of the mean evaporation source term $\widetilde{\rho}^{s}$ in the transport equation of the mean mixture fraction variance $\widetilde{Z}''^{2}$ (see eq. 5).

Fig.19 shows the comparison for a full load operation condition between combustion photographs taken from an optically accessible engine and numerical results. The optical engine represents a modern heavy duty truck engine. All relevant features of the optical engine are identical with a modern single cylinder engine test facility. Optical access is achieved with a special elongated transparent piston which contains a quartz window. The original piston bowl contour is machined into the quartz piston. The perspective of all combustion photographs in ***fig.19*** is from the bottom of the transparent piston. The luminescence can be associated with the soot radiation. The simulation results are plotted in form of temperature iso-surfaces with T=1400K since soot shows for it a yellowish shining which turns with upper temperatures into a white coloring. The overall agreement between simulation and diagnostic can be assessed as satisfactory. The progress of the combustion process is well predicted. Since the diagnostic photographs represent only single events and the calculation is ensemble-averaged, sub-structures of the experiments cannot be seen in the numerical results.

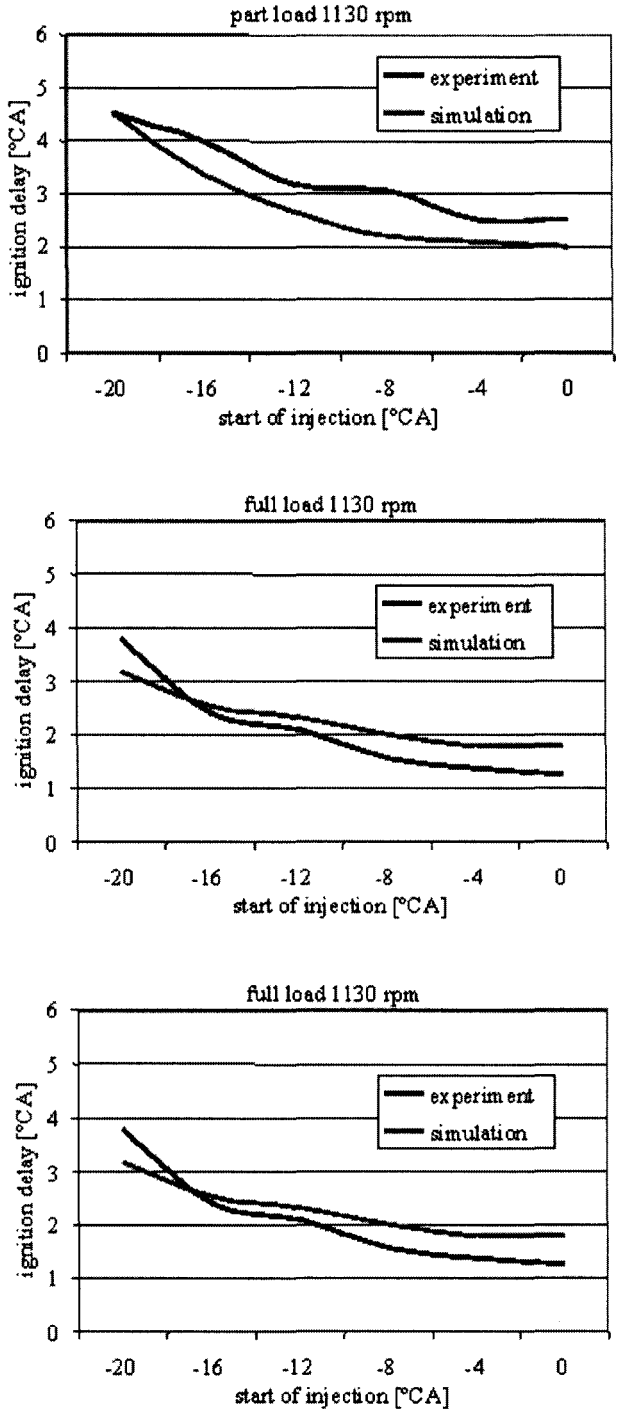

Figure 13: Comparison between simulated and measured ignition delays for the heavy duty truck engine.

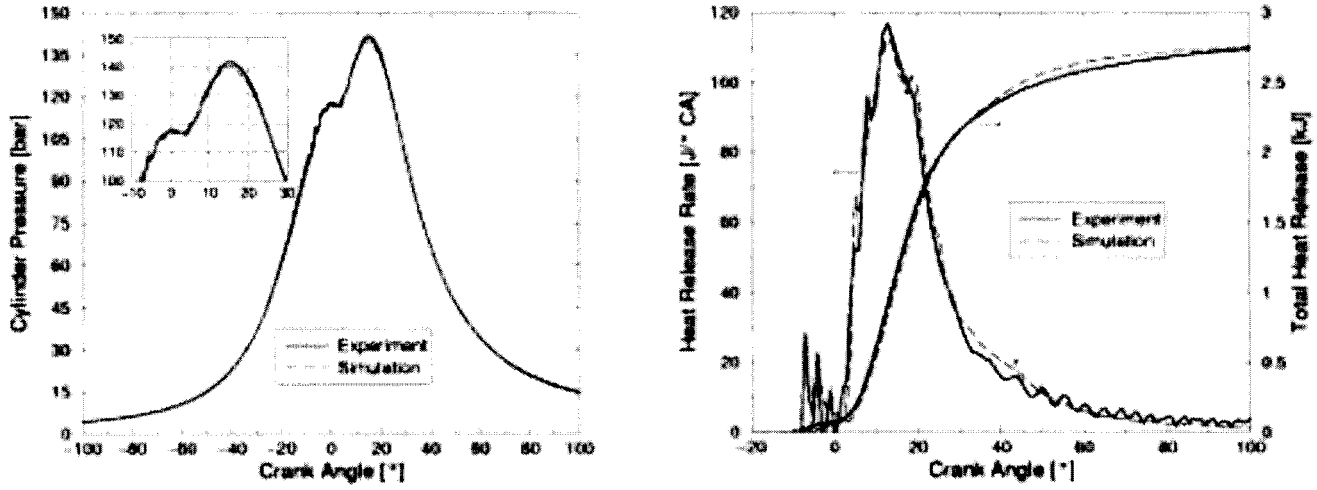

Figure 14: Comparison between measured and predicted traces of pressure, heat release and total heat release for the passenger car engine operating in full load mode with pilot injection.

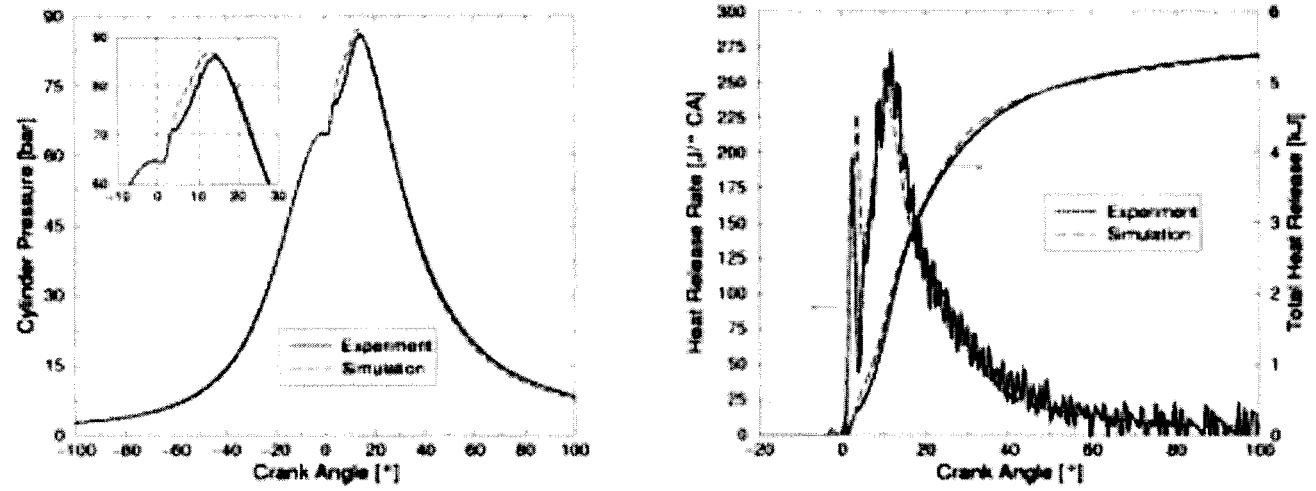

Figure 15: Comparison between measured and predicted traces of pressure, heat release and total heat release for the heavy duty truck engine operating in part load mode (SOI = 3bTDC).

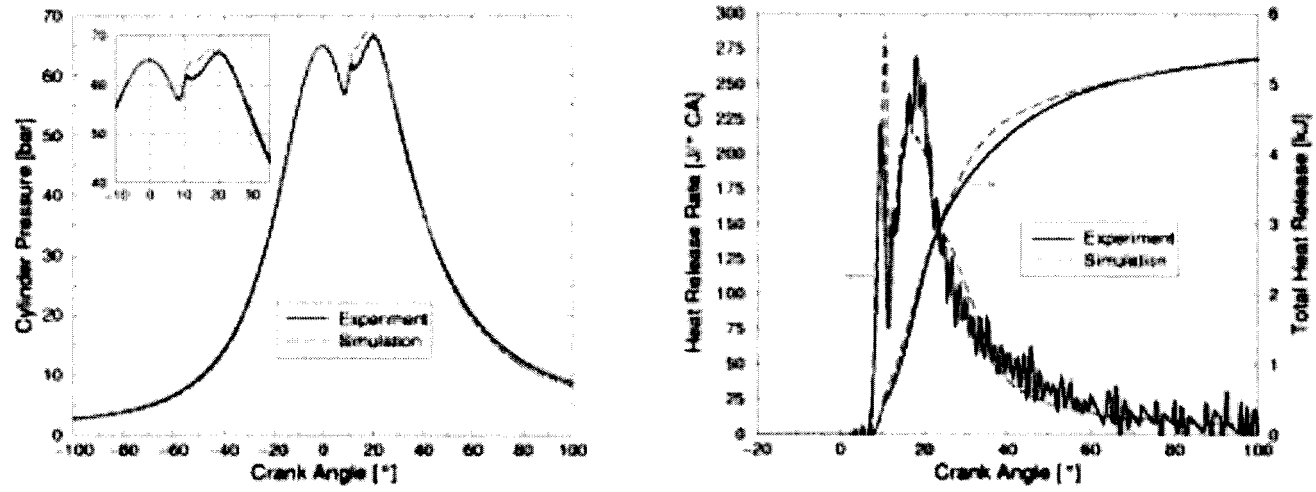

Figure 16: Comparison between measured and predicted traces of pressure, heat release and total heat release for the heavy duty truck engine operating in part load mode (SOI = 3aTDC).

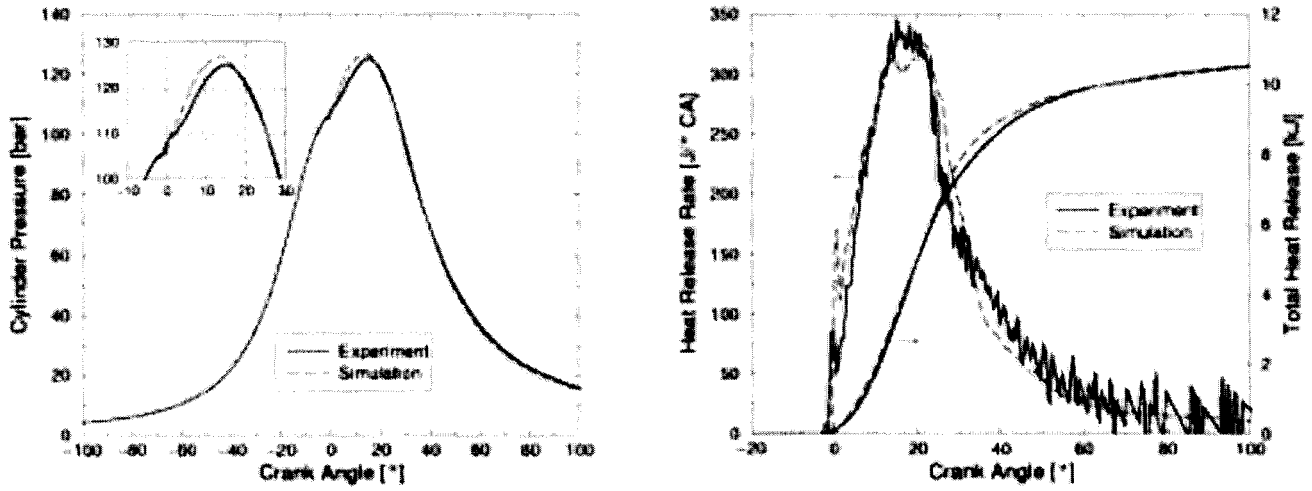

Figure 17: Comparison between measured and predicted traces of pressure, heat release and total heat release for the heavy duty truck engine operating in full load mode (SOI = 3bTDC).

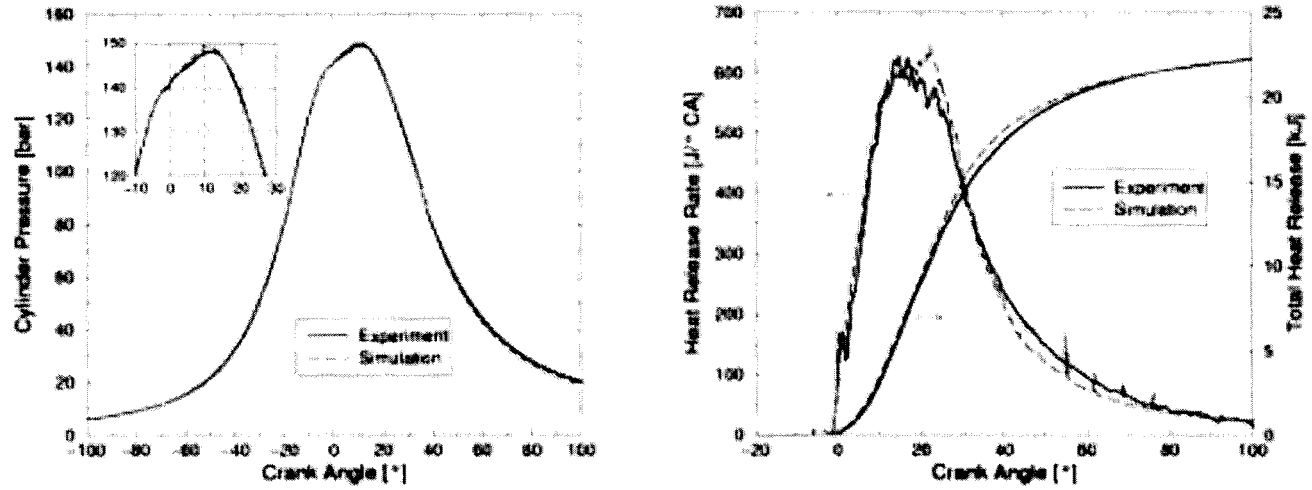

Figure 18: Comparison between measured and predicted traces of pressure, heat release and total heat release for the marine engine operating in full load mode (SOI = 3aTDC).

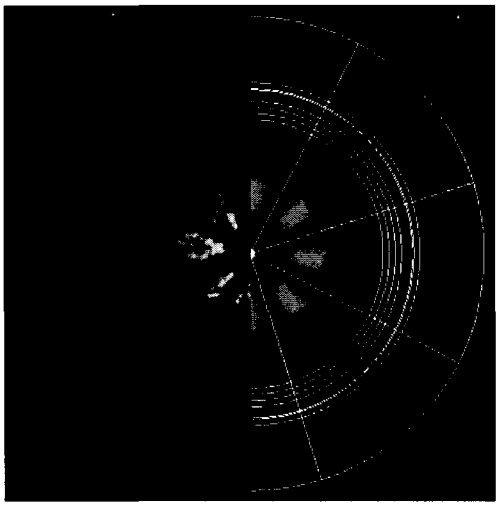

0.1° bTDC

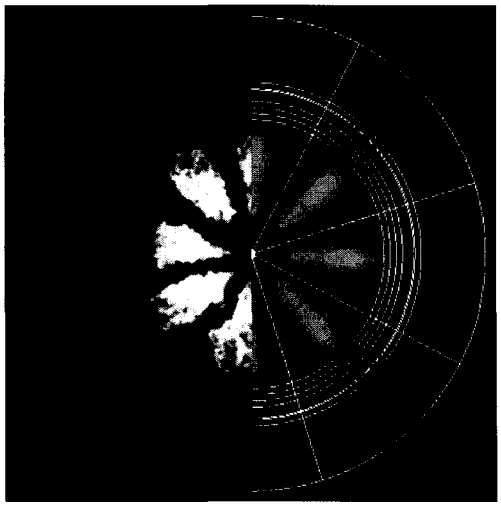

2.1° aTDC

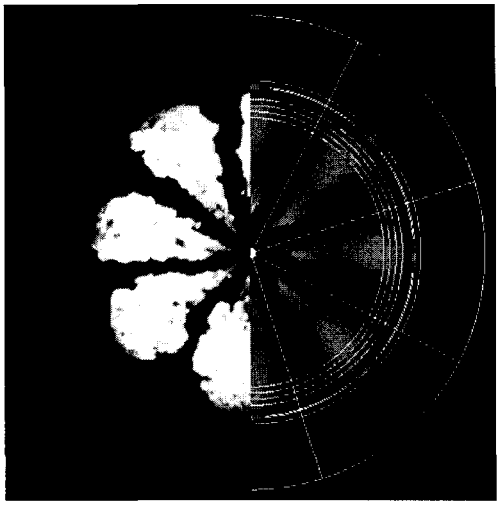

6.5° aTDC

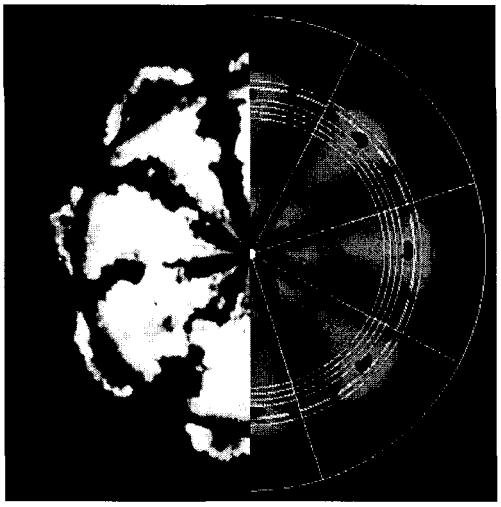

9.8° aTDC

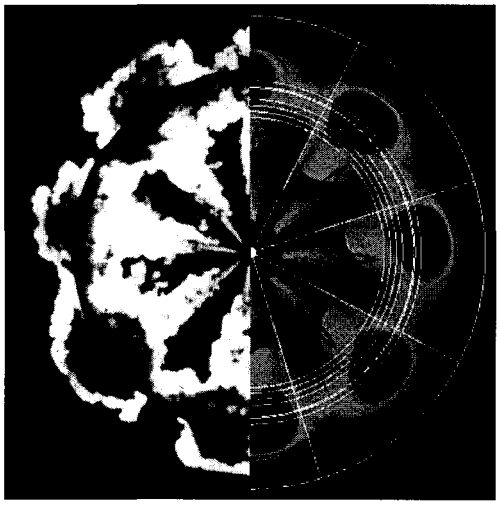

15.3° aTDC

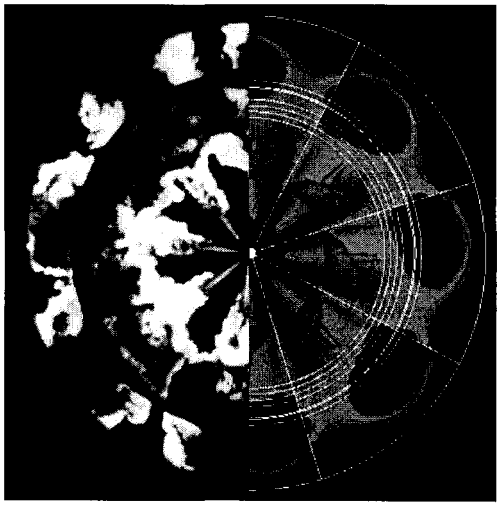

20.5° aTDC

Figure 19: Comparison between diagnostic and simulation for the heavy duty truck engine, full load case (mirrored view) (left: photographic sequence of the combustion cycle; right: calculated temperature iso-surface T=1400K)

CONCLUSION

In this paper an integrated numerical model for the simulation of internal combustion processes of DI Diesel engines has been introduced with the objective to meet the industrial demands of high degree of predictability and economical computational costs. For the spray modeling, an Eulerian model in combination with orifice resolving meshes and boundary conditions adapted from 3D simulations of the nozzle flow was applied. A progress variable approach for the simulation of the combustion process was used which subdivides into the phases of auto-ignition, premixed and diffusion combustion.

The present integrated model was used to simulate several different engines and operation conditions. The results show good agreement between experiment and simulation whereas most focus was put on the prediction of the heat releases.

The investigations reveal that the calculated premixed combustion phase tends to be slightly over-predicted. One reason for that is certainly based on the use of a simple empirical chemical time-scale approach. For a more realistic determination of the chemical time-scale, a new concept is introduced which allows the use of detailed reaction schemes. Additionally, an approach is presented which allows the prediction of HCCI ignition processes.

Making use of presumed pdf-methods for the closure of the reaction terms, the authors believe that further research is needed to improve the description of the pdf-shapes. Additionally, the influence of instantaneous local diffusion effects (→ scalar dissipation rate) on the ignition and combustion process has to be investigated.

REFERENCES

1. Krüger, C.: "Validierung eines 1D-Spraymodells zur Simulation der Gemischbildung in direkteinspritzenden Dieselmotoren", PhD Thesis RWTH Aachen, 2001.
2. Steiner, R., PhD Thesis in preparation.
3. Streule, T: "Dreidimensionale Simulation von Selbstzündung, Verbrennung und Schadstoffbildung in DE-Dieselmotoren", PhD Thesis Uni Karlsruhe, 2000.
4. Bauer, C., PhD Thesis in preparation.
5. Warnatz, J., Maas, U., Dibble, R.W.: "Combustion - Physical and Chemical Fundamentals, Modeling and Simulation, Experiments, Pollutant Formation" Springer-Verlag, 1996.
6. Peters, N.: "Laminar Diffusion Flamelet Models in Turbulent Non-Premixed Combustion", Prog Energy Combustion Sci., 10, 1984.
7. Peters, N.: "Turbulent Combustion", Cambridge Press, 2000.
8. Rao, S.: "A Probability Density Function Time-scale Model for Combustion Using Large Eddy Simulation", Master of Science Thesis, ERC Wisconsin-Madison, 2001.
9. Rao, S., Rutland, C.J.: "A Flamelet Timescale Combustion Model for Turbulent Combustion in KIVA", 12th Int. Multidim. Engine Modeling User's Group Meeting at the SAE Congress, 2002.
10. Kong, S.C., Han, Z., Reitz, R.D.: "The Development and Application of a Diesel Ignition and Combustion Model for Multidimensional Engine Simulation", SAE Paper 950278, 1995.
11. Reitz, R.D., Bracco, F.V.: "Global Kinetics Model and Lack of Thermodynamic Equilibrium", Combustion and Flame 53, 1983.
12. Press, W.H. et. al.: "Numerical Recipes in Fortran 77 The Art of Scientific Computing, Cambridge Press 1986-1992.
13. C. Krüger, F. Otto, F. Wirbeleit, J. Willand: " Incorporation of the Interactive Cross-Sectional Averaged Methodology for Diesel Spray Simulations into a 3D-Code", 9th International Multidimensional Engine Modeling User's Group Meeting at the SAE Congress, 1999.
14. N. Johnson, A. Amsden, J. Naber, D. Siebers: " Three-Dimensional Computer Modeling of Hydrogen Injection and Combustion", 95 SMC Simulation Multiconference, Phoenix, 1995.
15. G. König, M. Blessing, C. Krüger, U. Michels, V Schwarz: "Analysis of Flow and Cavitation Phenomena in Diesel Injection Nozzles and its Effects on Spray and Mixture Formation", 5th Internationales Symposium für Verbrennungs-diagnostik der AVL Deutschland, Baden-Baden 2002.
16. F. Otto, C. Krüger, F. Wirbeleit, J. Willand: " Probleme und Lösungsansätze bei der Simulation

der dieselmotorischen Einspritzung, Meß- und Versuchstechnik für die Entwicklung von Verbrennungsmotoren", Haus der Technik, Essen 1999.
17. Nehse, M., Warnatz, J., Chevalier, C.: "Kinetic Modeling of the Oxidation of Large Aliphatic Hydrocarbons", 26th Symposium (Int.) on Combustion, The Combustion Institute, Pittsburgh, 1996.
18. Westbrook, C.K.: "Chemical Kinetics of Hydrocarbon Ignition in Practical Combustion Systems", Proceedings of the Combustion Institute, Volume 28, 2000.
19. Abraham, J.: "What is Adaquate Resolution in the Numerical Computations of Transient Jets", SAE Paper 970051, 1997.
20. Wan, Y., Peters, N.: "Scaling of Spray Penetration with Evaporation", Atomization and Sprays Vol.9, 1999.
21. Amsden, A.A., O`Rourke, P.J., Butler, T.D.: "KIVA-II: A Computer Program for Chemically Reactive Flows with Sprays", Los Alamos Report LA-11560-MS, Los Alamos National Laboratory, 1989.
22. Krüger, C., Steiner, R., Krauss, E., Otto, F.: "Demands on CFD Models of Mixture Preparation and Combustion in IC Engines for Industrial Purposes", 5th World Congress on Computational Mechanics, 2002.

APPENDIX

A SEMI-ANALYTICAL β-PDF INTEGRATION

For the numerical solution of the integral

$$\tilde{\psi}_i(\vec{x},t) = \int_Z \psi_i(Z)\tilde{P}_Z(Z;\vec{x},t)dZ \quad , \qquad \text{(A1)}$$

where ψ_i represents any flamelet solution and $\tilde{P}_Z$ the Favre β-pdf, in this appendix a semi-analytical method is introduced. The β-pdf inserted in eq. A1 gives:

$$\tilde{\psi}_i = \gamma \int_Z \psi_i \cdot Z^{\alpha-1}(1-Z)^{\beta-1}dZ \qquad \text{(A2)}$$

The normalization factor γ is calculated by the complete β-function which itself is related to the gamma-function Γ so it can be determined analytically:

$$\gamma = \left(\int_{Z=0}^{Z=1} Z^{\alpha-1}(1-Z)^{\beta-1}dZ \right)^{-1} = \frac{\Gamma(\alpha)\cdot\Gamma(\beta)}{\Gamma(\alpha+\beta)} \qquad \text{(A3)}$$

Typically, the flamelet solutions ψ_i are given in form o tables, i.e. in discrete manner. Assuming linear functions in these sub-intervals, the discrete problem of eq. A2 turns into a functional expression:

$$\tilde{\psi}_i = \gamma \sum_{n=1}^{N-1} \int_{Z_n}^{Z_{n+1}} (m\cdot Z + c)_{[n,n+1]} \cdot Z^{\alpha-1}(1-Z)^{\beta-1}dZ \qquad \text{(A4)}$$

where N is the total number of grid points. For the solution of eq. A4 the incomplete β-function can be usec which describes the integration in the interval [0,x]:

$$B(x,a,b) = \gamma \int_{Z=0}^{Z=x} Z^{\alpha-1}(1-Z)^{\beta-1}dZ \qquad \text{(A5)}$$

For its numerical evaluation, e.g. in **[12]** an algorithm is given, which is based on a continued fractior representation.